- Technical Paper -

EFFECT OF MIX DESIGN AND CURING CONDITION ON TRAPPED AIR BUBBLES DURING WATER PERMEATION

Hanjing LIN[*1], Yuya SAKAI[*2]

ABSTRACT

During liquid water permeation into concrete, air trapping occurs and may affect water mass transport. To determine the relationship between the amount of trapped air bubbles, mix design, and curing condition, water absorption tests of different mortar and cement paste mixtures with different air-entrainment agent usage, water to cement ratios, fly ash/blast furnace slag proportions, and curing were conducted under decompression and atmospheric conditions. Air trapping estimates were affected by mix design and curing condition, but not directly correlated with porosity.

Keywords: air bubbles, water permeation, penetration depth, mix design, mortar, cement paste, porosity

1. INTRODUCTION

Concrete is a porous material, and water permeation into concrete is closely related to the pore structure of the concrete. When water is absorbed into hardened concrete by capillary forces, some air is trapped in the process [1]; this phenomenon has been proven to manifest and exist during capillary water filling via nanochannel observation [2].

Trapped air bubbles during water infiltration can cause discrepancies between the theoretical quantitative evaluations of water migration in concrete and actual permeated water volume [3]. Moreover, such air trapping may also affect the durability of the concrete structure, for example, its resistance against the freezing and thawing cycles, chloride ion penetration, and so on. Sakai et al. [4] compared cement paste specimens with different amounts of trapped air bubbles and observed that those with more air bubbles showed less or even no damage after approximately one hundred freeze–thaw cycles. Regarding chloride ion diffusion and transport in concrete materials, most theoretical and numerical models in existence assume the concrete pore to be saturated after water permeation; however, if trapped air bubbles remain in the water infiltration route, concrete may be partially unsaturated in reality, and there may be gaps between the calculated and actual diffusion processes. To reduce such evaluation gaps and clarify the mechanism of water permeation, this study focused on trapped air bubbles.

By using degassed water instead of tap water for the water infiltration tests, concrete specimens were observed to absorb a greater quantity of water [2], which suggested that the amount of air along with different initial experimental settings, such as initial air quantity in the water, affect the amount of trapped air bubbles and water permeation. Besides, it was indicated that pore structure also affects air trapping in hardened cement paste during water transport as a result of the ink-bottle geometry, which was observed by Sakai et al. [4]. Fagerlund [5] explained that in the capillary water absorption process, the trapped air bubbles are under pressure and are compressed and dissolved to some extent; the enclosed air pressure inside these air bubbles provide resistance against surface tension. Thus, as is schematically illustrated in Fig. 1, owing to different in-pore air resistances, the amount of absorbed water in specimens under decompression or vacuum conditions are likely to be greater than that under atmospheric pressure. Accordingly, such differences are estimated herein to determine the amount of trapped air bubbles.

Different types of binders and water-to-binder ratios create different pore structures; thus, the amount of trapped air bubbles may be affected by binders and water-to-binder ratios (W/B) [5]. The admixtures frequently added into concrete nowadays, such as fly ash (FA) and blast furnace slag (BFS) were chosen as binders in this study. It has been often indicated that air-entrainment agents (AEAs) can cause significant changes to the microstructures of cement pastes and to its pore structures, in particular, even with small usage amounts [4-6]. According to the AEA manual adopted in this research, different quantities of AEAs were added to the mortar and cement paste specimens as one variable. In the mix design, curing of the specimens is also an important factor; thus, different curing conditions,

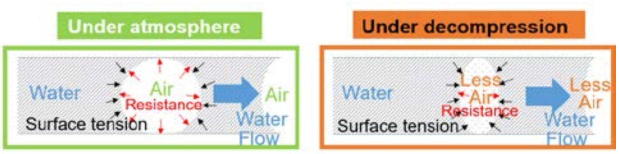

Fig. 1 Schematic illustration of capillary water filling under atmosphere or decompression condition

*1 Graduate School of Engineering, the University of Tokyo, JCI Student Member
*2 Assistant Prof., Institute of Industrial Science, the University of Tokyo, Dr.E., JCI Member

Table 1 Material properties

Type	Specifications
Cement	Ordinary Portland cement (Density: 3.15 g/cm^3, Specific surface area: 3510 cm^2/g)
Sand	Fujigawa river sand (Surface dry density: 2.62 g/cm^3, FM: 2.55)
Admixture material	Fly ash (Density: 2.21 g/cm^3, Blain value: 3400 cm^2/g) Blast furnace slag (Density: 2.91 g/cm^3, Blain value: 4250 cm^2/g)
Admixture chemical	AE agent (Alkyl ether series, Density: 1.04 g/cm^3)

including water curing, sealed curing, and air curing, were applied to different specimens. Combining all parameters in the mix design mentioned above, water absorption tests of mortar specimens and cement paste specimens mixed pertinently were conducted to understand the qualitative relationship between the parameters in the mix design and air trapping during water permeation.

To discuss the relationship between the permeable pores of specimens and the amount of trapped air bubbles during absorption tests, porosity tests were also conducted on the cement paste specimens afterwards.

2. TEST PROGRAMS

2.1 Materials and Mix Proportions

The properties of some common construction materials are shown in Table 1. The prepared mortar and cement paste specimens were cylinders of 5-cm diameter and 10-cm height. The main mix variables were the water-to-cement ratio (W/C), usage of AEA and admixtures, and curing condition.

(1) Mortar

Nine different mortar mixtures were prepared as shown in Table 2, where the specimens named as M50-1, M50-2, and M50-3 differed in curing conditions and M50-4, M50-5, and M50-6 differed in the usage of AEAs. The air content was measured for freshly mixed mortar using JIS A 1116 method, and the results were 4–6% of the air-entrained mortar volume, which was in accordance with JSCE standard.

(2) Cement paste

Fifteen cement paste mixtures were prepared as shown in Table 3, where the specimens named as P50-1, P50-2, and P50-3 differed in curing conditions, P50-4 to P50-8 differed in the usage of AEAs, and F50-1, F50-2 were mixed by respectively replacing 20% and 40% cement with FA by weight, and B50-1, B50-2 were mixed by respectively replacing 30% and 60% cement with BFS by weight.

2.2 Sample Preparation and Conditioning

The specimens were demolded 24 h after casting, cured according to mix design tables for 28 d, and dried at 40 °C and 30% relative humidity (RH) until the masses were stable. Each mix was cast for two samples for water absorption tests under atmospheric and decompression conditions. The curing and tests were mainly conducted at 20 °C and 60% RH environment.

Before drying, the samples prepared for water absorption tests were cut into slices of 4-cm thickness by a water-cooling cutter 2 cm away from the casting surface and 4 cm away from the bottom of the samples to avoid non-uniformities due to water bleeding. For mortar specimens, after the water absorption tests, water penetration depths were measured; for the cement paste samples, porosity tests were conducted to investigate the factors that dominate air trapping.

Table 2 Mix design for mortar mixes

Name	W/C	Curing	Mass per unit volume (kg/m^3)			AEA (mL/kg C)
			W	C	S	
M35	0.35	Water	324	925	2117	2.5
M45	0.45	Water	392	871	2117	2.5
M55	0.55	Water	453	823	2117	2.5
M50-1	0.5	Water	423	847	2117	2.5
M50-2	0.5	Sealed	423	847	2117	2.5
M50-3	0.5	Air	423	847	2117	2.5
M50-4	0.5	Water	423	847	2117	2
M50-5	0.5	Water	423	847	2117	3.5
M50-6	0.5	Water	423	847	2117	5

Table 3 Mix design for cement paste mixes

Name	W/B	Curing	Mass per unit volume (kg/m^3)			AEA (mL/kg C)
			W	C	FA or BFS	
P30	0.3	Water	486	1620	-	-
P40	0.4	Water	558	1394	-	-
P50	0.5	Water	612	1223	-	-
P50-1	0.5	Water	612	1223	-	-
P50-2	0.5	Sealed	612	1223	-	-
P50-3	0.5	Air	612	1223	-	-
P50-4	0.5	Water	612	1223	-	2
P50-5	0.5	Water	612	1223	-	3
P50-6	0.5	Water	612	1223	-	3.5
P50-7	0.5	Water	612	1223	-	4
P50-8	0.5	Water	612	1223	-	5
F50-1	0.5	Water	592	947	237	-
F50-2	0.5	Water	574	688	459	-
B50-1	0.5	Water	606	848	363	-
B50-2	0.5	Water	600	480	720	-

2.3 Water Absorption Tests

The amount of trapped air bubbles during water permeation was analyzed by comparing water absorption masses under atmospheric and decompression conditions with two samples prepared beforehand to absorb water from their bottom sides. Here, two different water absorption experimental methods were adopted for the mortar and cement paste samples. For the mortar samples, not only were the absorption masses measured after the water absorption tests but water penetration depths were also measured to evaluate the relationship between penetration depth and water absorption amount.

(1) Mortar

For the mortar specimens, every time one sample was absorbing water under atmospheric pressure, the other one was absorbing water under decompression condition inside a vacuum glove box, as presented in Fig. 2, which was set to -82 kPa by a vacuum pump. By monitoring the crane used to move the samples upwards or downwards, the sample inside the box was allowed to begin and end absorption at the same time as the one outside. The original amounts of water in the containers were set to about 1.5 cm depth, and the absorption time duration was fixed as 2 h so that different absorption results, including absorption masses and penetration depths, were likely to manifest between the two samples. After the 2-hour absorption and measuring masses, the two samples were cut into two halves to measure the penetration depth using the spraying water detector on the split surfaces.

(2) Cement paste

For the cement paste specimens, similarly, two samples of one series were used every time, as presented in Fig. 3; samples shown on the left were absorbing water under atmospheric condition, whereas the other one was absorbing water inside the desiccator following ASTM vacuum saturation technique, where the pressure was set to -90 kPa [8] by vacuum pump evacuation. To decrease probable errors caused by human and system factors during experiment operations, all ϕ 5×4 cm cement paste cylinder specimens listed in Table 3 were divided into four different groups based on the variables in the mix design, including W/C group (P30, P40, P50), curing condition group (P50-1, P50-2, P50-3), AEA group (P50-4 to P50-8), and FA/BFS group (F50 and B50); in one absorption test, all specimens from the same group were picked at one time, for example, in Fig. 3, 2×8 samples from FA/BFS group and 2×5 samples from AEA group were chosen to absorb water simultaneously. First, half of the selected samples were vacuum saturated by placing in the desiccator as shown in Fig. 3 under -90 kPa pressure for 3 h, and then back-filing with enough prepared degassed water to entirely cover all the samples under vacuum so that no air can invade inside; meanwhile, the other half of the samples were placed in a bucket exposed to air to absorb tap water from this moment. Unlike the amount of the tap water restored in the bucket, after all the samples were located, nearly all samples were immersed but the boundary surfaces in the top were safe from water so that there remained one route for the trapped air bubbles to get away during water permeation. Then, one additional hour later, the stopcock for the desiccator was opened so that the air was allowed to enter inside until the inner pressure reached atmospheric condition, and the stopcock was closed again so that all the specimens were soaked under water under atmospheric pressure. In total, for vacuum saturated specimens in the desiccator, vacuum operation lasted for 4 h. After 20 more hours, all the samples were removed from the water, and the masses of the different samples were measured after suction.

The reason why the former water absorption test method was adopted for mortar rather than the vacuum saturation method was to invalidate the explanation that larger suction masses under decompression condition were due to faster water permeation rates with lower pressures. For cement paste specimens, the commonly used vacuum saturation tests were applied. Longer suction times in the latter approach allows water to penetrate throughout the cement paste samples after vacuum saturation in the desiccator or after 21-hour water suction under atmospheric condition.

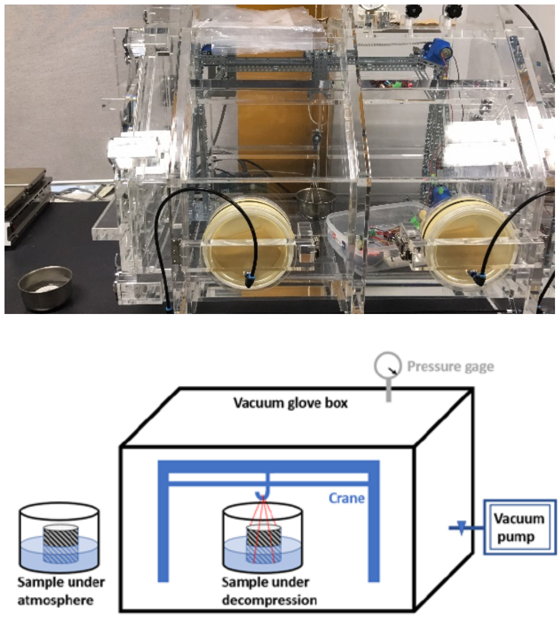

Fig. 2 Photo and simplified schematic model of water absorption test – mortar

(a) Atmospheric pressure

(b) Decompression

Fig. 3 Photo of water absorption test - cement paste

2.4 Porosity Tests

To justify whether different trapped air bubbles occurring in water absorption tests were influenced by the different permeable pore volumes of specimens mixed with different mix designs, after completing vacuum saturation, porosity tests were conducted on the cement paste samples, which were tested under decompression condition. The surface-dry masses and the buoyant masses of the saturated samples were measured with a gravity measurement kit after saturation, and the samples were dried at 105 °C for more than 48 h to obtain the oven-dry masses. Eventually, according to the calculations for the weight gain due to water absorption and weight loss due to buoyancy, the permeable porosity was computed by equation Eq. 1 as follows:

$$\text{Permeable porosity} = (W_s-W_d) / (W_s-W_b)\times 100\% \quad (1)$$

where,

W_s: buoyant mass of saturated sample in water

W_d: oven-dry mass of sample in air

W_b: saturated surface-dry mass of sample in air

3. TEST RESULTS

3.1 Water Penetration Depth

The results of water penetration depths in case of mortar specimens are presented in Fig. 4 combined with the test results of their water suction masses. The horizontal axis lists all the mortar specimens in Table 2 in sequence from left to right; the differences of penetration depths between two specimens in same water absorption test but under decompression and atmosphere conditions are expressed by grey bars; the differences between their suction masses are plotted in orange bars. These differences were calculated by subtracting values under atmospheric pressure from those under decompression condition and all of them are greater than zero.

It was evident that the differences between suction masses were not always rising responding to the penetration depth difference increase, which excluded the possibility that penetration depth is the cause of different water suction masses and suggested that it is appropriate to apply the common method vacuum saturation tests herein. Accordingly, it is also reasonable to assume that the amount of different trapped air bubbles can affect the water permeation process and the values of the above orange bars can show the amount of trapped air bubbles.

3.2 Water Absorption Mass

The first vertical axes of the following figures were obtained by calculating the differences between decompression conditions and atmosphere conditions of water suction masses of mortar specimens as introduced in Fig. 4; the second vertical axes described the differences between two pressure conditions of water suction masses divided by initial masses of cement paste specimens. The suction mass of mortar was not divided by the initial mass because specimens were not saturated after the test, and the initial masses were different in each specimen due to the difference in the height. In this research, these two kinds of values were used to estimate the amount of trapped air bubbles.

(1) Air-entrainment agent

As presented in Fig. 5, the horizontal axis is for different usages of AEA. For mortar, AEA usages located at 2, 2.5, 3.5, 5 mL/kg cement; and for cement paste specimens, AEA usages located at 0, 2, 3, 3.5, 4, 5 mL/kg cement.

The above results obtained by mortar and cement paste specimens all indicated that smallest amount of trapped air bubbles can occur somewhere from 2.5 to 4 mL/kg cement; and when usage of AEA was 2 mL/kg cement, largest amounts of air bubbles were trapped within the present designed range.

(2) Curing condition

As presented in Fig. 6, the horizontal axis was about different curing conditions, from left to right, the results were about mortar and cement paste specimens cured in the water, sealed and in the air.

Both the results of mortar and cement paste specimens suggested that air curing causes more trapped air bubbles than other two curing conditions, however, not too explicit tendency appeared between specimens with water curing condition and sealed curing condition from present results by mortar and cement paste specimens.

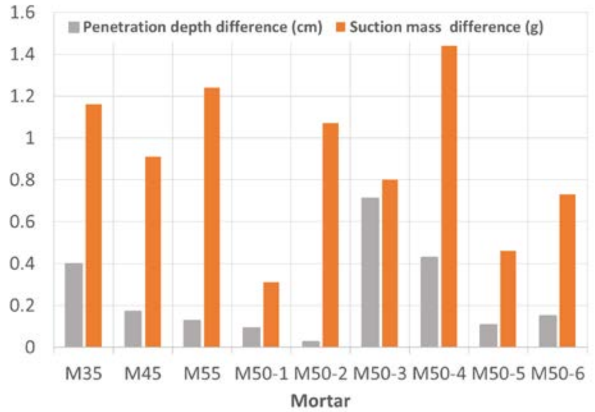

Fig. 4 Comparison of penetration depth differences and suction mass differences

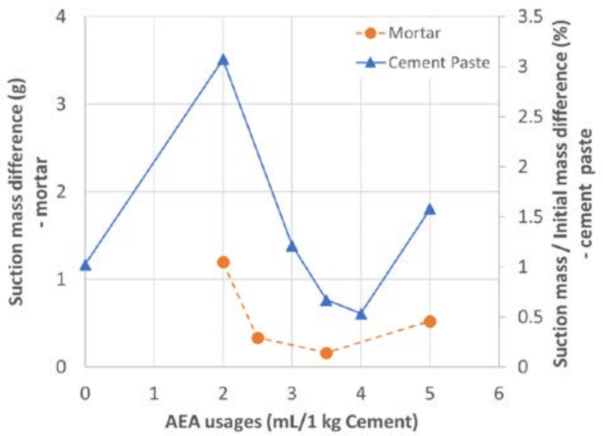

Fig. 5 Different usages of AEA

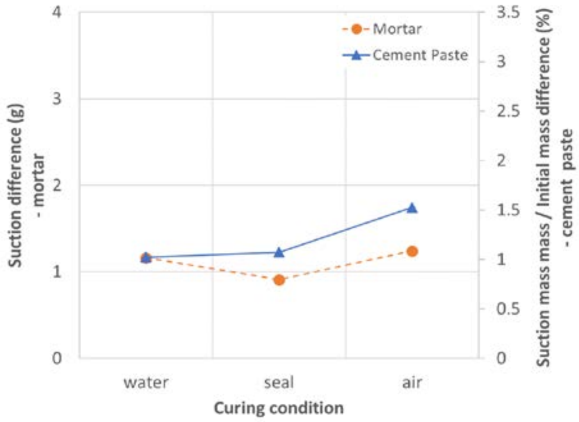

Fig. 6 Different curing conditions

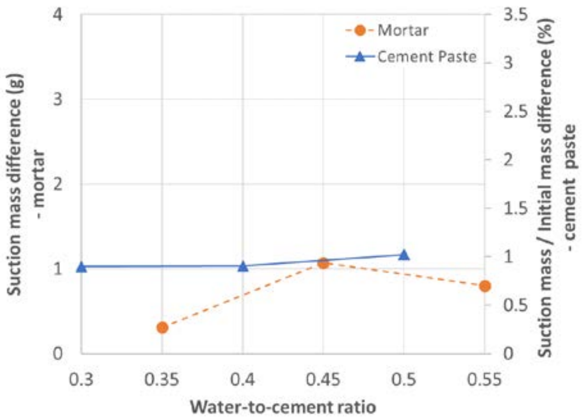

Fig. 7 Different water-to-cement ratios

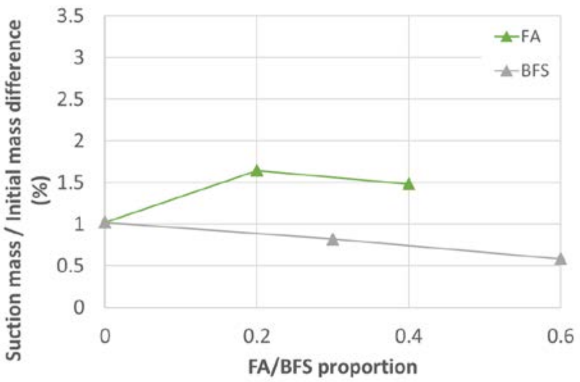

Fig. 8 Different proportions of FA/BFS

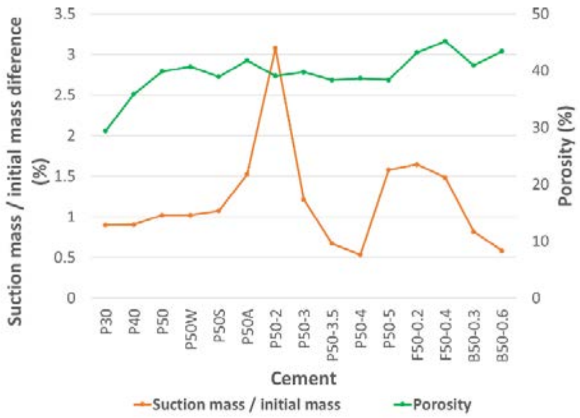

Fig. 9 Comparison of porosity and different suction mass/initial mass of cement paste

(3) Water-to-cement ratio

As presented in Fig. 7, the horizontal axis was about different water-to-cement ratios. For mortar, W/C located at 0.35, 0.45, 0.55; and for cement paste specimens, water-to-cement ratios located at 0.3, 0.4 and 0.5.

Above two lines showed within designed water-to-cement ratios in this research, there indicated no clear and definite connections between water-to-cement ratios and amount of air trapping.

(4) Fly Ash/Blast Furnace Slag

As described in Fig. 8, the horizontal axis was about different proportions of FA or BFS for cement paste specimens. For FA, proportions located at 0, 0.2, 0.4; for BFS, proportions located at 0, 0.3, 0.6.

With fly ash added into the binders of cement paste, the estimation of trapped air bubbles increased within certain range and then decreased, for instance in this research, at the proportion of 0.2, most air trapping was examined. However, after blending with certain proportions of blast furnace slag, air bubbles were estimated to be trapped less.

3.3 Porosity

The porosity of tested cement paste specimens listed in Table 3 was summarized in Fig. 9 coupling with the results of their water absorption tests as sequenced in the horizontal axis.

As present above, two lines changed rather differently, and there indicated no direct correlations. Therefore, it required further research work to investigate what factors will dominate when trapping air bubbles during liquid water permeation into concrete, for instance, pore size distributions.

Furthermore, the porosity plots were around 40% and the amounts of measured trapped air bubbles was 3% in cement paste at largest as shown in Fig. 9. Assuming the porosity of cement paste as 40%, these trapped air bubbles correspond to 7.5 % (=0.03/0.4) of absorbed water, which is not nominal or negligible. However, it is probable that the vacuum saturation cannot remove all trapped air bubbles, therefore, the actual amount of the trapped air bubbles is likely to be larger than this value. The effect on the trapped air bubbles on concrete durability needs to be discussed in detail for more accurate estimation of concrete durability.

4. CONCLUSIONS

(1) The amount of trapped air bubbles showed variously and always, under decompression condition with lower pressure, mortar and cement paste specimens absorbed more water than under atmosphere condition. These differences were assumed to be one kind of reasonable evaluations

for air trapping.

(2) Mortar and cement paste specimens mixed with different mix designs including different usages of AEAs, W/C and BFS/FA proportions, and different curing conditions were filled with water in pores differently during water absorption tests. The results obtained by far indicated that specimens with certain amount of AEAs, specimens blended with FA and specimens cured in the air trapped larger amount of air bubbles during water permeation.

(3) There was no direct relationship between porosity and amount of trapped air bubbles. Combining with porosity test results, air trapping estimates obtained in this study were proven to be not negligible.

ACKNOWLEDGEMENT

This research was financially supported by Japan Concrete Institute.

REFERENCES

[1] Hall, C., & Hoff, W. D., “Water Transport in Brick, Stone and Concrete,” CRC Press, 2004, pp. 221-226.

[2] Chauvet, F., et al. “Roles of Gas in Capillary Filling of Nanoslits,” Soft Matter, 8.41, 2012, pp. 10738-10749.

[3] Sakai, Y., & Kishi, T., “Quantitative Evaluation of Water Migration in Concrete with Threshold Pore Diameter Obtained Based on Critical Volume Fraction for Percolation,” Journal of Japan Society of Civil Engineers, Ser. E2 (Materials and Concrete Structures), Vol. 72, 2016, pp. 83-96.

[4] Sakai, Y., Kamada, T., & Kishi, T., “Freezing Damage Mechanism in Model Microchannels and Vacuum Curing on Cement Paste to Improve Frost Damage Resistance,” Concrete Research and Technology, Vol. 28, 2017, pp. 15-24.

[5] Fagerlund, G., “The Long Time Water Absorption in the Air-pore Structure of Concrete,” Lund Unveristy, Lund Institute of Technology, Division of Building Materials, 1993, pp. 9-15.

[6] Wong, H. S., et al., “Effect of Entrained Air Voids on the Microstructure and Mass Transport Properties of Concrete,” Cement and Concrete Research, Vol. 41, Oct. 2011, pp. 1067-1077.

[7] Sun, Z., & Scherer, G. W., “Effect of Air Voids on Salt Scaling and Internal Freezing,” Cement and Concrete Research, Vol. 40, Feb. 2010, pp. 260-270.

[8] Safiuddin, M., & Hearn, N., “Comparison of ASTM Saturation Techniques for Measuring the Permeable Porosity of Concrete,” Cement and Concrete Research, Vol. 35, May 2004, pp. 1008-1013.

[9] Japan Society of Civil Engineers (JSCE). “Standard Specification for Concrete Structures.” Materials and Construction, 2007.